PCEE 2019
NEW ZEALAND SOCIETY FOR EARTHQUAKE ENGINEERING
2019 Pacific Conference on Earthquake Engineering
TURNING HAZARD AWARENESS INTO RISK MITIGATION
4 – 6 April | SkyCity, Auckland | New Zealand
nzsee

Predicting low-cycle fatigue life of buckling-restrained braces

B. Saxey & Z. Vidmar
CoreBrace, LLC/West Jordan, Utah, United States

C-H. Li, M. Reynolds & C-M. Uang
Department of Structural Engineering/University of California, San Diego, United States

ABSTRACT

Fifteen buckling-restrained braces (BRBs) were tested at the University of California, San Diego (UCSD). Of the fifteen specimens there existed 3 discrete groupings of 5 nominally identical specimens. The three groups represent 3 different strength levels of BRBs. Each brace was subjected to either constant-strain amplitude cycles, variable-amplitude symmetric cycles, or simulated earthquake loading until fracture of the steel core occurred. Within each group a range of constant-strain amplitudes cycles was chosen. The objective of the research was to investigate the low-cycle fatigue behaviour of BRBs and to develop a predictive low-cycle fatigue model for seismic applications.

1 INTRODUCTION

Extensive research including system-level testing has demonstrated that buckling-restrained braced frame (BRBF) is a reliable seismic force-resisting system. As a result, BRBF has gained worldwide acceptance for new construction or seismic retrofit of buildings and other structures. BRBFs are expected to provide significant inelastic deformation capacity primarily through buckling-restrained braces (BRBs). Under seismic loading, the steel core of a BRB yields in tension and develops a high-mode local buckling mode in compression to also force steel yielding. The fatigue life assessment of BRB is of interest to engineers since a decision can be made on whether BRBs must be replaced after an earthquake. In this study, a series of fatigue tests on fifteen BRBs have been conducted. A BRB low-cycle fatigue life assessment method is developed based on the test results.

2 TEST PROGRAM

Three sets of five nominally identical BRB specimens for a total of 15 specimens were tested at the Caltrans Seismic Response Modification Device (SRMD) test facility at UCSD. The three sets, series A, B, and C, had incrementally larger core cross-sectional areas (A_{sc}) with an expected yield strength (P_{ye}) of 1110, 2220, and 3330 kN, respectively. The brace core plates and steel casing were manufactured with A36 and A500 Gr. B steel, respectively. Table 1 depicts the test matrix. The first number, 1110, 2220, or 3330 in the specimen designation represents the value of P_{ye}.

Within each set, three braces were cyclically tested to fracture with constant-amplitude of ±0.25%, ±0.75% and ±2.0% core strains, respectively. In addition, there was one specimen in the B series that was tested with a ±3.0% constant-amplitude. For these constant-amplitude test specimens, a number 0.25, 0.75, 2.0, or 3.0 was appended to the specimen designation. To simulate the strain rate effect expected in an earthquake, cyclic testing was conducted in a dynamic manner such that the imposed strain rate reached around 0.75%/s for ±0.25% cycle tests and as high 5.0%/s for the other constant-amplitude cycle tests.

Two specimens were imposed with the variable-amplitude symmetric cycles during the test. Specimen 1110-S1 was tested with a modified AISC loading protocol. The AISC loading protocol, prescribed in Section K3 of the AISC Seismic Provisions (AISC 2016), was modified such that the repeated constant cycles at the end of the loading protocol was not performed. Instead, the ramped 5 discrete strain levels of the AISC protocol (±0.15%, ±0.5%, ±1.0%, ±1.5% and ±2.0%), which were performed for two cycles each, were repeated until the specimen failed. Specimen 3330-S2 was subject to a two-phase constant-amplitude test. It was first subjected to a total of 1,000 cycles of ±0.25% constant-amplitude strain before ±0.75% constant-amplitudes cycles were applied until fracture. The "S" in the designation for these two specimens represents that the imposed cycles are symmetric.

The fifth BRB specimen in each set was subjected to simulated earthquake responses that were repeated until fracture. These specimens were designated with "EQ". To generate the strain histories for simulated earthquake loading, nonlinear time-history analyses were performed on an example 4-story BRBF (4F-BRBF) building in the AISC Seismic Design Manual (AISC 2018). The nonlinear structural analysis software PISA3D (Lin *et al*. 2009) was used for the analyses.

Table 1: Test matrix

Series	**Test Specimen Designation**	**BRB Properties** A_{sc} (mm^2)	P_{ye} (kN)	L_b (mm)	**Constant Amplitude Tests**	**Variable Amplitude Tests**
A	1110-0.25	3,652	1,110	5,477	±0.25%	-
	1110-0.75				±0.75%	-
	1110-2.0				±2.00%	-
	1110-S1				-	Modified AISC Protocol
	1110-EQ1				-	Simulated Earthquake^1
B	2220-0.25	7,232	2,200	5,461	±0.25%	-
	2220-0.75				±0.75%	-
	2220-2.0				±2.00%	-
	2220-3.0				±3.00%	-
	2220-EQ2				-	Simulated Earthquake^2
C	3330-0.25	11,135	3,300	5,424	±0.25%	-
	3330-0.75				±0.75%	-
	3330-2.0				±2.00%	-
	3330-S2				-	Two-phase Constant-Amplitude
	3330-EQ3				-	Simulated Earthquake^3

1. 1989 Loma Prieta (120% MCE) and 1999 Hector Mines (100% MCE)
2. 1994 Northridge (100% MCE)
3. 1989 Loma Prieta, 2016 Amberley (NZ), and 1985 Michoacán (Mexico) (All three are scaled to100% MCE)

For Specimen 1110-EQ1, the simulated core strain history was obtained from the first-story BRBs in the example frame with a 1989 Loma Prieta earthquake record scaled to 120% of the maximum considered earthquake (MCE) level and a record form the 1999 Hector Mine earthquake scaled to the MCE level. The loading sequence for Specimen 2220-EQ2 was generated from a record from the 1994 Northridge earthquake scaled to the MCE Level. For producing Specimen 3330-EQ3 loading sequence, three ground motions scaled to the MCE level were used. They were records from the 1989 Loma Prieta, 2016 Amberley (New Zealand), and 1985 Michoacán (Mexico) Earthquakes. The values of the spectral response acceleration parameters S_{DS} = 1.0 and S_{D1} = 0.6 were used to define MCE.

3 TEST RESULTS

Table 2 summarizes the constant-amplitude tests results. It can be found that, generally, the BRB fatigue lives under the ±0.25%, ±0.75% and ±2.0% strain amplitude were approximately 2,000, 200 and 20 cycles, respectively. Based on the limited test data, the BRB constant-amplitude fatigue life would be less than 10 cycles for the ±3.0% strain.

Figure 1 shows the measured axial displacement time history of a test specimen (Specimen 2220-0.25). For high-capacity braces that required a large number of cycles at lower strain amplitude (±0.25% and ±0.75% in this program), testing had to be conducted at intervals due to the hydraulic system limitations of the SRMD test facility. The figure shows that the entire fatigue test for Specimen 2220-0.25 was completed by 12 test runs. Except for the first trial test run and the last test run in which the rupture occurred, each of the other test runs had 220 cycles. During each test run, the imposed strain amplitude gradually decreased in the first half and maintained relatively constant in the second half of the run. As the figure shows, however, the mean strain amplitude in the both tension and compression were very close to the target strain amplitude (0.25% in this case).

Figure 2 shows the sample hysteretic responses of the B Series specimens under the constant-amplitude tests. Table 2 also lists the normalized cumulative inelastic deformation (η_D) for the constant-amplitude test specimens. The normalized total inelastic axial deformation for a cycle with a deformation level greater than the yield deformation is given by:

$$\mu_i = \frac{2|\Delta_i^+ - \Delta_i^-|}{\Delta_{by}} - 4 \tag{1}$$

Table 2: Constant-amplitude test results

Series	Specimen Designation	Target Strain Amplitude (%)	Target Strain Range (%)	Number of Cycles to Failure	Normalized Inelastic Deform., η_D
A	1110-0.25	±0.25	0.5	2,072	5,573
B	2220-0.25			2,346	6,780
C	3330-0.25			2,278	6,719
A	1110-0.75	±0.75	1.5	201	3,346
B	2220-0.75			174	2,867
C	3330-0.75			243	3,957
A	1110-2.0	±2.0	4.0	16	808
B	2220-2.0			22	1126
C	3330-2.0			31	1542
B	2220-3.0	±3.0	6.0	9	687

where Δ_i^+ and Δ_i^- are the values of the maximum and minimum deformations for the i^{th} cycle, respectively, and Δ_{by} is the BRB deformation corresponding to the yielding of the brace. The deformation-based cumulative inelastic axial deformation, η_D, is then calculated as the summation of the normalized inelastic axial deformation for each cycle:

$$\eta_D = \sum \mu_i \tag{2}$$

For uniaxial testing of BRBs, the AISC Seismic Provisions (AISC 2016) require that the cumulative normalized inelastic deformation (η_D) reach a value of at least 200. The value of η_D of those ±0.25% strain specimens could reach 5,600 to 6,800. The ±0.75% strain specimens withstood a η_D value ranging from 2,900 to 4,000. Under the ±2.0% cycles, the specimens sustained a η_D around 800 to 1,500. When the strain amplitude was increased to ±3.0%, the BRB still developed a η_D of 687.

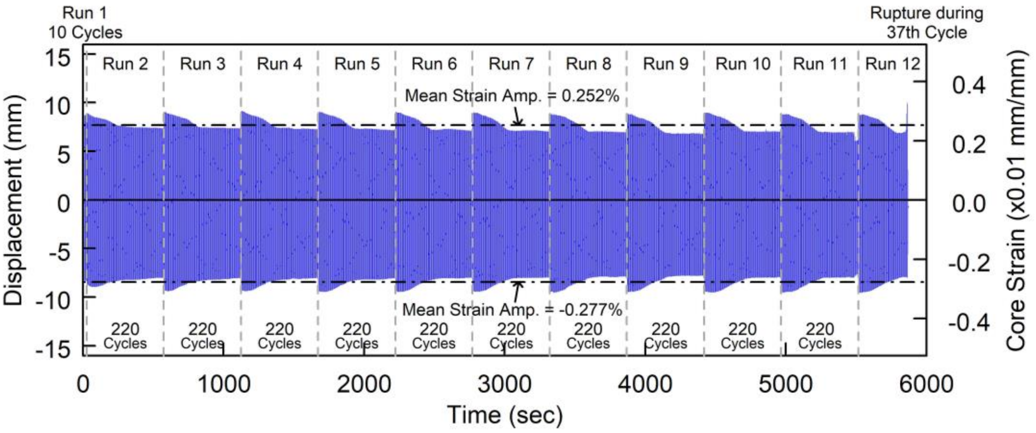

Figure 1: Sample axial displacement history (Specimen 2220-0.25)

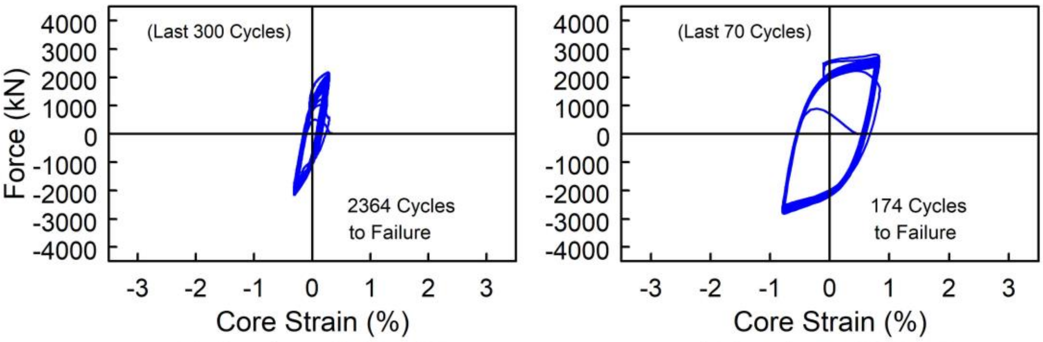

(a) Specimen 2220-0.25

(b) Specimen 2220-0.75

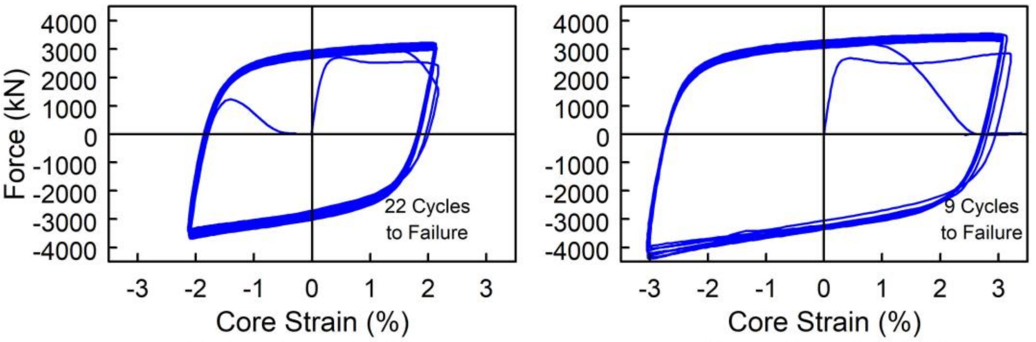

(c) Specimen 2220-2.0

(d) Specimen 2220-3.0

Figure 2: Hysteretic responses of B series specimens (constant-amplitude tests)

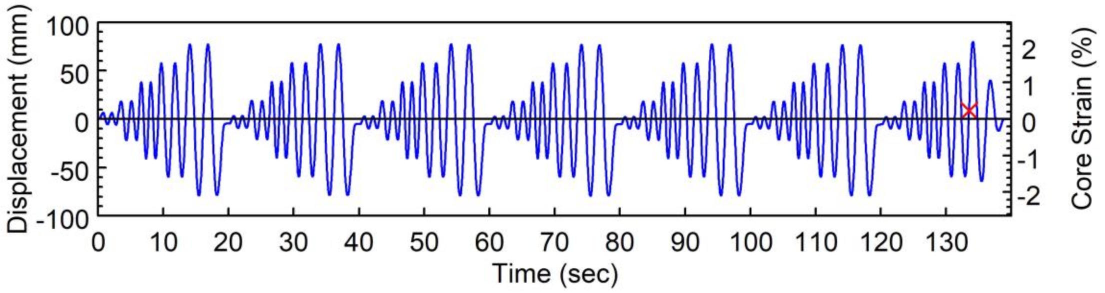

(a) Specimen 1110-S1 (Modified AISC Loading Sequence)

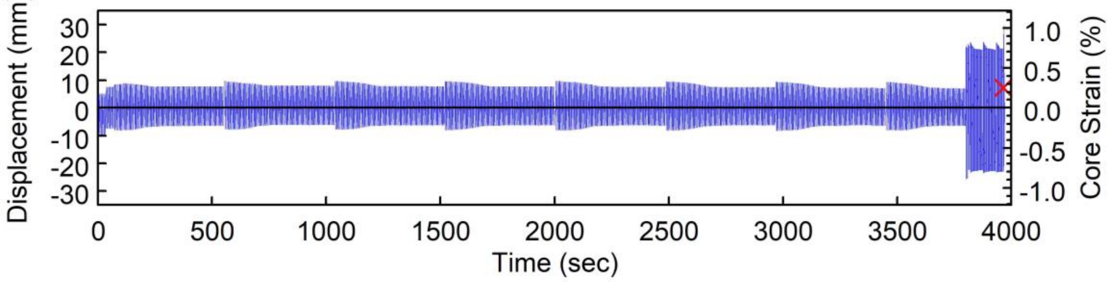

(b) Specimen 3330-S2 (Two-Phase Constant-Amplitude Loading Sequence)

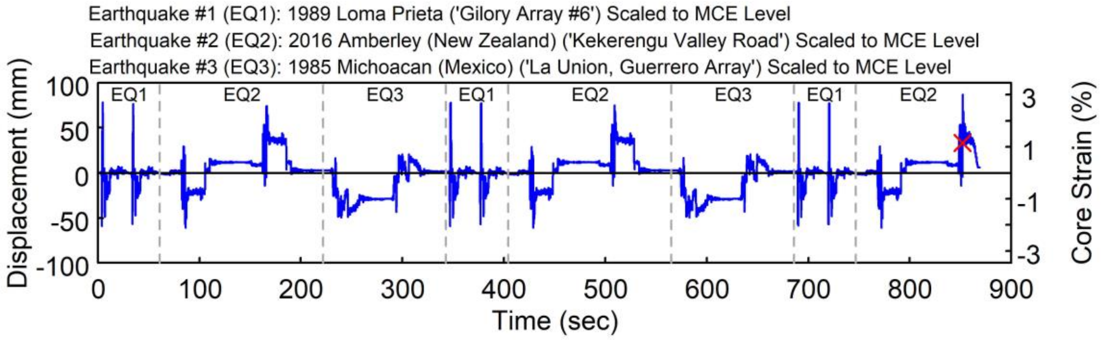

(c) Specimen 3330-EQ3 (Simulated Earthquake Loading Sequence)

Figure 3: Displacement time histories of variable-amplitude tests: (a) Specimen 1110-S1; (b) Specimen 3330-S2, and (c) Specimen 3330-EQ3

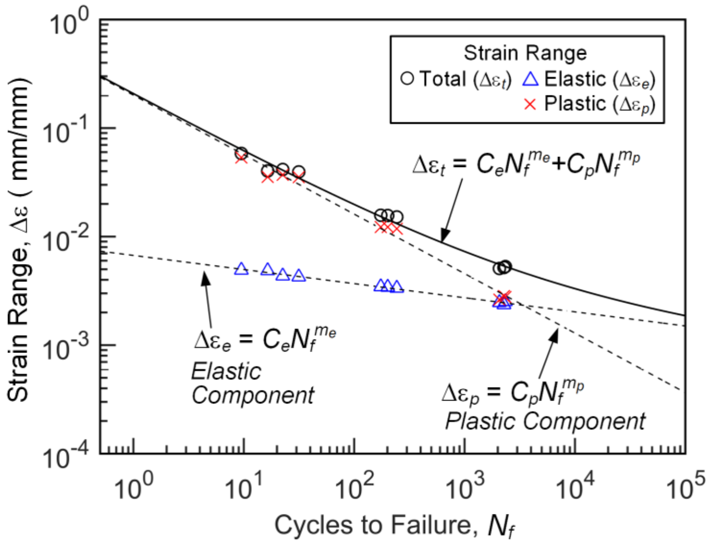

Figure 4: Fatigue curves based on constant-amplitude test results

Figure 3 shows core strain time histories of sample variable amplitude tests. Specimen 1110-S1 completed 6 test runs of modified AISC protocol and fractured during the tension excursion of the first 2.0% cycle of the 7th test run (Figure 3a). The η_D reached 1,580. Specimen 3330-S2 first completed 1,000 cycles of ±0.25% target core strain amplitude and then withstood 113 cycles of ±0.75% strain amplitude before fracture (Figure 3b). The specimen developed a η_D value of 5,033, of which the ±0.25% strain-amplitude cycles contributed 62.5% of the η_D and the ±0.75% cycles contributed the remaining. Figure 3c shows the displacement time of Specimen 3330-EQ3. For those earthquake loading tests, Specimens 1110-EQ1, 2220-EQ2, and 3330-EQ3 generated η_D values of 1,584, 1,592, and 998, respectively. It is noted that each of these three specimens survived the simulated MCE response more than 10 times.

4 LOW-CYCLE FAIGUE LIFE PREDICTION MODEL

The constant-amplitude test results were used to establish a low-cycle fatigue life assessment model. The procedure used for establishing the fatigue model for the base metal (Raske and Morrow 1969) was adopted herein for the BRBs. The average core strain, ε, is defined as Δ_b/L_y, where Δ_b and L_y are measured brace displacement and the length of the steel core plate in the yielding zone, respectively. For each half cycle of the hysteresis loops, the total strain range ($\Delta\varepsilon_t$), was separated into the elastic ($\Delta\varepsilon_e$) and plastic ($\Delta\varepsilon_p$) components. The total strain range, $\Delta\varepsilon_t$, was the strain excursion from the tension to compression strain peaks or that from compression to tension strain peaks. In addition, the average stress of the BRB core was calculated by dividing the brace axial force by A_{sc}. The elastic strain range component, $\Delta\varepsilon_e$, was obtained by dividing the absolute stress amplitude difference between the tension and compression strain peaks by the Young's modulus, E. Finally, the plastic component, $\Delta\varepsilon_p$, was computed as $\Delta\varepsilon_t - \Delta\varepsilon_e$.

Considering the results of all ten constant-amplitude tests, Figure 4 shows that the relationship between the elastic strain range, $\Delta\varepsilon_e$, and the number of cycles to failure (N_f) could be approximated by a linear relationship in a log-log plot. The same linear trend was also observed between the plastic strain range, $\Delta\varepsilon_p$, and N_f. Regression analyses were conducted to establish the relationships between both the elastic and plastic strain ranges and the number of cycles to failure, which yield the following results:

$$\Delta\varepsilon_e = C_e {N_f}^{m_e} = 0.0067{N_f}^{-0.13} \tag{3}$$

$$\Delta\varepsilon_p = C_p {N_f}^{m_p} = 0.2012{N_f}^{-0.55} \tag{4}$$

where C_e and m_e are the constants for the $\Delta\varepsilon_e$ versus N_f relationship, and the C_p and m_p are for the $\Delta\varepsilon_p$ versus N_f relationship. Then the fatigue model relating the total strain range to the number of cycles to failure was:

$$\Delta\varepsilon_t = \Delta\varepsilon_e + \Delta\varepsilon_p = C_e {N_f}^{m_e} + C_p {N_f}^{m_p} = 0.0067{N_f}^{-0.13} + 0.2012{N_f}^{-0.55} \tag{5}$$

where $\Delta\varepsilon_t$, $\Delta\varepsilon_e$, and $\Delta\varepsilon_p$ are in mm/mm, not % of mm/mm.

The variable strain amplitude test results were used to verify the effectiveness of the low-cycle fatigue model. The rain-flow counting method (Matsuishi and Endo 1968) was employed for the variable-amplitude tests to extract the number of cycles and their respective strain range. After applying the rain-flow counting, the entire loading history could be analysed as a series of full-cycles and a series of half-cycles. Each full-cycle or half-cycle has its own corresponding total strain range, $\Delta\varepsilon_t$. The rain-flow counting results were then used in the calculation of the Miner's damage index, D (Miner 1945). The proposed calculation method is:

$$D = \sum_{i=1}^{n} \frac{n_i}{N_{fi}} = \sum_{j=1}^{N_{full}} \frac{1}{N_{fj}} + \frac{1}{2}\left[\sum_{k=1}^{N_{half}} \frac{1}{N_{fk}}\right] \tag{6}$$

where

$$\begin{aligned} \Delta\varepsilon_{tj} &= 0.0067{N_{fj}}^{-0.13} + 0.2012{N_{fj}}^{-0.55} \\ \Delta\varepsilon_{tk} &= 0.0067{N_{fk}}^{-0.13} + 0.2012{N_{fk}}^{-0.55} \end{aligned} \tag{7}$$

where N_{full} and N_{half} are the numbers of full-cycles and half-cycles, respectively. $\Delta\varepsilon_{tj}$ and $\Delta\varepsilon_{tk}$ represent the strain ranges corresponding to the *j*-th full-cycle and the *k*-th half-cycle, respectively. Equation (7), which comes from the proposed low-cycle fatigue model in Eq. (5), gives the predicted number of cycles to failure, N_{fj} and N_{fk}, corresponding to the strain ranges $\Delta\varepsilon_{tj}$ and $\Delta\varepsilon_{tk}$, respectively. The strain excursion of a full-cycle of strain range $\Delta\varepsilon_{tj}$, was assumed to generate a *D* value of $1/N_{fj}$ and the strain excursion of a half-cycle of strain range $\Delta\varepsilon_{tk}$ would consume a fatigue life of $1/(2N_{fk})$. Summing the results for all strain excursions within a loading sequence produces the Miners Damage index (D) per equation (6). A value of *D* reaching 1.0 means the BRB would fracture.

Table 3: D-indices for constant-amplitude test specimens

Target Strain Amplitude	Series	Specimen Designation	*D*-index	Average *D*-index	Coefficient of Variation (COV)
0.25%	A	1110-0.25	0.76	0.87	11.9%
	B	2220-0.25	0.97		
	C	3330-0.25	0.89		
0.75%	A	1110-0.75	1.18	1.18	12.8%
	B	2220-0.75	1.03		
	C	3330-0.75	1.33		
2.00%	A	1110-2.0	0.67	0.96	29.5%
	B	2220-2.0	0.98		
	C	3330-2.0	1.24		
3.00%	B	2220-3.0	0.82	-	-
			Avg. = 0.99 COV = 21.6%		

Table 4: D-indices for variable amplitude test specimens

Loading Type	Series	Specimen Designation	*D*-index	Average *D*-index	Coefficient of Variation (COV)
Symmetric Cycles with Variable Amplitude	A	1110-S1	1.04	1.05	2.5%
	C	3330-S2	1.07		
Simulated Earthquake Response	A	1110-EQ1	1.18	0.95	25.0%
	B	2220-EQ2	0.96		
	C	3330-EQ3	0.71		
			Avg. = 0.99 COV = 18.0%		

Based on the proposed calculation procedure, Tables 3 and 4 list the *D* values for the constant- and variable-amplitude test specimens, respectively. A *D*-index smaller than 1 represents that the BRB specimen ruptured earlier than the prediction. On the other hand, a *D*-index larger than 1 means that the BRB ruptured later than the prediction. For the constant-amplitude tests, the *D*-index ranges from 0.67 to 1.33. The proposed method tends to overestimate the fatigue life for the ±0.25% strain tests and underestimate those of the ±0.75% strain tests. The coefficients of the variation (COV) of *D*-index for these two groups of specimens were about 12%. For the ±2.0% strain tests, the COV of *D*-index is 29.5%, suggesting that the variation of the fatigue performance would increase with the strain amplitude.

Table 4 shows that the *D*-indices for the variable amplitude tests range from 0.71 to 1.18. This is within the variation range observed from the constant-amplitude tests. Also note that the average value and COV of the *D*-indices are similar to those from the constant-amplitude tests. For the two symmetric loading tests with variable-amplitudes, Specimens 1110-S1 and 3330-S2, the *D*-indices are very close to 1, indicating that the proposed method predicts the failure very well for this type of loading history. For the earthquake loading test specimens, the prediction method still works reasonably well. The *D*-indices for Specimens 1110-EQ1, 2220-EQ2, and 3330-EQ3 are 1.18, 0.96, and 0.71, respectively, although the prediction method somehow overestimates the fatigue life of Specimen 3330-EQ3. It is expected that this level of accuracy is sufficient to provide practicing engineers with the information necessary to recommend reuse or replacement of a BRB after an earthquake if the displacement history of the BRB is known.

5 CONCLUSIONS

Test results showed that BRB specimens had a fatigue life much larger than the code requirements. A low-cycle fatigue model has been calibrated from the constant-amplitude tests results in this research. The variable-amplitude tests results have verified that the proposed fatigue model together with the Miner's damage index could assess the remaining fatigue life of BRBs under earthquake-generated loading to a reasonable accuracy.

REFERENCES

American Institute of Steel Construction (AISC). 2016. *Seismic Provisions for Structural Steel Buildings*, ANSI/AISC 341-16. AISC Chicago, IL.

American Institute of Steel Construction (AISC). 2018. *Seismic Design Manual*, 3rd Edition. AISC, Chicago, IL.

Lin, B.Z., Chuang, M.C. & Tsai, K.C. 2009. Object- oriented Development and Application of a Nonlinear Structural Analysis Framework, *Advances in Engineering Software*, Vol 40(1) 66-82.

Matsuishi, M. & Endo, T. 1968, Fatigue of Metals Subjected to Varying Stress, *Japan Society of Mechanical Engineers*, Jukvoka, Japan.

Miner, M.A. 1945. Cumulative damage in fatigue, *Journal of Applied Mechanics*, Vol 12 159-164.

Raske, D.T. & Morrow, J. 1969. Mechanics of Materials in Low Cycle Fatigue Testing, *Manual on Low Cycle Fatigue Testing*, Vol 465 1-25, ASTM STP.

Tavernelli, J.F. & Coffin, L.F. 1962. Experimental Support for Generalized Equation Predicting Low Cycle Fatigue, *Journal of Basic Engineering*, Vol 84 533-537, ASME.